ELSEVIER

Soil Dynamics and Earthquake Engineering 24 (2004) 537–550

SOIL DYNAMICS AND EARTHQUAKE ENGINEERING

www.elsevier.com/locate/soildyn

Seismic behaviour of flexible retaining systems subjected to short-duration moderately strong excitation

G. Gazetas*, P.N. Psarropoulos, I. Anastasopoulos, N. Gerolymos

School of Civil Engineering, National Technical University Athens, Greece

Accepted 20 February 2004

Abstract

Using finite-element modelling, this paper explores the magnitude and distribution of dynamic earth pressures on several types of flexible retaining systems: L-shaped reinforced-concrete walls, piled walls with horizontal or with strongly inclined anchors, and reinforced-soil walls. The utilized base excitation is typical of earthquake motions of either high or moderately low dominant frequencies having a peak ground acceleration (PGA) of 0.40 g and relatively short duration. Linear as well as non-linear (Mohr–Coulomb) soil behaviour is investigated, under dry conditions. The results show that, as the *degree of realism* in the analysis increases, we can explain the frequently observed satisfactory performance of such retaining systems during strong seismic shaking.

Keywords: Retaining walls; Reinforced-concrete walls; Anchored walls; Reinforced-soil walls; Piled walls; Seismic behaviour

1. Introduction

The performance of retaining walls during earthquakes has been found to depend profoundly on the existence of water and the presence of loose cohesionless soils in the supported soil and the foundation. Experimental studies and earthquake reality have shown that harbour quay-walls, made up either of caisson gravity walls or, especially, of passively anchored sheet-pile walls, are quite vulnerable to strong seismic shaking, mainly as a result of strength degradation of saturated cohesionless soils in the backfill and the foundation. This vulnerability was amply demonstrated in the 1995 Kobe earthquake, as well as many previous and subsequent earthquakes [3,7–10,21,32].

Such behaviour is contrary to the behaviour of flexible retaining walls such as the semi-gravity type L-shaped Reinforced-Concrete (LRC) walls, Prestressed-Anchor Piled (PAP) walls, and Reinforced-Soil (RS) walls, retaining non-saturated cohesionless soils or saturated clayey soils. These type of walls have behaved particularly (and sometimes surprisingly) well during many recent earthquakes: Loma Prieta (1989), Northridge (1994), Kobe (1995), Chi-Chi (1999), Kocaeli (1999), and Athens (1999) earthquakes. This, despite the fact that they had been designed for base accelerations of almost 20% of the peak ground accelerations which they actually experienced in the earthquake.

Three categories of methods of analysis are currently used in practice for such walls: one category, by far the most popular, are the pseudo-static limit-equilibrium based methods of the Mononobe–Okabe (M-O) method type [17,19].

The second category are the linear or equivalent-linear visco-elasticity based methods which use either analytical [31] or numerical tools for arriving at a solution. The third category, which also enjoys some limited popularity for flexible walls, models the 'active' and 'passive' soil reaction through Winkler-type non-linear springs [26].

The objective of this paper is to present a numerical study of the dynamic stresses imposed on a variety of retaining systems, under short-duration and impulsive base excitation, in order to unveil some of the salient causes of their excellent behaviour. The soil is modelled as both elastic and inelastic material, and in this way we bridge the gap between limit-equilibrium and elasticity solutions.

The optimistic results obtained from our analyses are corroborated with Kerameikos metro station case history from the 1999 Athens (Parnitha) earthquake, as well as with experimental observations.

* Corresponding author. Fax: +30-210-7722028.

0267-7261/$ - see front matter © 2004 Published by Elsevier Ltd.
doi:10.1016/j.soildyn.2004.02.005

2. Retaining systems examined

Despite their structural simplicity, retaining walls are rather complicated soil-structure-interaction systems, the dynamic response of which has not yet been fully understood. This paper addresses the dynamic behaviour of three different types of retaining structures:

(a) L-shaped Reinforced-Concrete (LRC) walls, having different degrees of flexural rigidity and founded either on bedrock or top of a relatively deep soil layer of parametrically variable stiffness.
(b) Prestressed-Anchor Piled (PAP) walls or Prestressed-Anchor Diaphragm (PAD) walls, with horizontal or inclined anchors, and
(c) Reinforced-Soil (RS) walls, characterized by the density and size of the steel reinforcement, and the rigidity of the wall face.

This paper first highlights observations of the field performance of a variety of such walls during the Kobe, Chi-Chi, Kocaeli, Northridge, and Athens earthquakes, thus documenting their satisfactory behaviour even under extremely strong seismic shaking. Then, it presents graphically the results of the numerical studies for some representative examples of such walls.

3. Observed behaviour of retaining walls in recent earthquakes

Retaining systems supporting non-saturated soils have performed well during many recent earthquakes. Here are few examples:

In the 1995 M_w 7 Kobe earthquake a wide variety of retaining structures was put to test [12,13,28–30]. Most of them were located along the railway lines of the city. Gravity-type retaining walls, such as masonry, unreinforced concrete, and leaning type, were heavily damaged. Surprisingly, however, reinforced-concrete walls experienced only limited damage. Several LRC walls (in Rokko-michi, Ishiyagawa, and Shioya) although subjected to long-period accelerations with peak values perhaps as high as 0.80 g, were only moderately damaged. Similarly, geosynthetic reinforced-soil (RS) walls were only slightly damaged. One such wall in Tamata, subjected to a peak-ground-acceleration (PGA) of about 0.80 g, experienced some sliding and tilting, while a similar one in Tarumi showed only limited deformation. Another CRC wall, near Tamata, supported on bored piles, was also only slightly damaged.

In the 1999 M_w 7.6 Chi-Chi Taiwan earthquake, flexible reinforced-concrete walls, as well as reinforced-soil (RS) retaining walls also performed well [15]. However, there was a significant difference, which led to some exceptions. RS retaining walls in Kobe were equipped with full height rigid facings. In contrast, RS walls in Taiwan had non-rigid facings of precast-concrete blocks, connected to the geogrid reinforcement with pins. In some cases, where the vertical spacing of reinforcement was too large, the lower part of the facing experienced localized bulging and collapse, in a few cases leading to total failure. The failure can be attributed to the larger earth pressures that the lower part of the facing was subjected to, which led to bulging deformation and rupture or pull-out of the pins. At Chang-Chiun Park, near the fault, RS retaining walls with a vertical reinforcement spacing between 60 and 80 cm experienced only slight damage, while those with vertical spacing of 120 cm were severely damaged, exhibiting large residual deformations.

In the 1999 M_w 7.5 Kocaeli earthquake, two twin 10-m high RS wing walls of the Arifiye Bridge overpass were located on top of the North Anatolian fault, next to lake Sapanca [16,20]. The walls consisted of square interlocking reinforced concrete facing panels (side of 150 cm), of ribbed galvanized steel strips 40 mm × 50 mm in cross-section spaced at 90 cm, and well compacted sand-gravel backfill. Despite the strong ground shaking, and the large fault-rupture displacement, no significant damage was observed.

In the 1994 M_w 6.8 Northridge earthquake numerous 'temporary' anchored walls (in active construction sites) were subjected to acceleration levels in excess of 0.20 g—in some cases as large as 0.60 g. Lew et al. [14] describe four such PAP walls in greater Los Angeles, with excavation depths ranging from 15 to 25 m, and retaining more-or-less stiff soils. In all cases the measured deflections of the walls did not exceed a mere 1 cm, and of course there was no visual change attributable to seismic shaking.

Finally, at the time of the 1999 M_S 5.9 Athens (Parnitha) earthquake several metro stations were being constructed. Among these stations particularly interesting is the case of the Kerameikos metro station [5]. The retaining structure of the station had essentially not been designed against earthquake. However, although subjected to nearly 0.50 g PGA, no damage was visible after the earthquake. The maximum wall displacement was estimated to have been of the order of a few centimeters.

4. L-shaped reinforced-concrete (LRC) walls: seismic deformation and pressures

Among the three categories of examined walls, the semi-gravity type L or T shaped reinforced-concrete walls appear to be the most sensitive, but still have performed satisfactorily during earthquakes. Despite their seeming simplicity, analysis of their dynamic response has proved a difficult task, owing to the complicated pattern of outward displacements that such walls may undergo and the ensuing inelastic soil behaviour. The displacement pattern involves four types of motion, illustrated in Fig. 1:

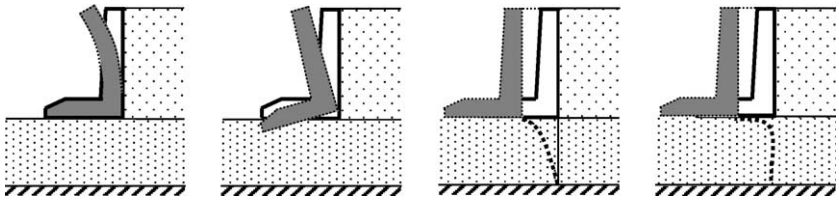

Fig. 1. Possible modes of displacement of an L-shaped wall: (a) structural flexure, (b) base rotation, (c) elastic base translation, and (d) inelastic base translation (sliding).

(a) flexural deformation of their stem
(b) elastic and inelastic rigid-body rotation of their footing (base)
(c) elastic horizontal translation of their footing (base)
(d) sliding at their footing (base).

While explicitly accounting for all these motions is a formidable task, for over 70 years practical seismic analysis of retaining walls has been based on a pseudo-static extension of Coulomb's limit-equilibrium analysis—the widely known Mononobe–Okabe method. Modified and simplified by Seed and Whitman [27], the method has prevailed thanks to its simplicity and the familiarity of engineers with the (static) Coulomb method. In its simplest form, the Seed and Whitman version gives the seismic force, ΔP_{AE}, and its point of application as follows:

$$\Delta P_{AE} \approx \frac{1}{2}\gamma H^2\left(\frac{3}{4}\alpha_o\right) = 0.375(\alpha_o \gamma H^2)$$

$$h_{AE} \approx 0.6H$$

where $\alpha_o(=A_o/g)$ is the peak ground acceleration (presumed to be unique in space).

In practice, h_{AE} was often taken as $0.5H$, leading to the simplified interpretation of ΔP_{AE} as the resultant force of a uniform pressure

$$\sigma_{AE} \equiv \sigma = 0.375(\alpha_o \gamma H)$$

Experimental studies in the 60s and 70s using small-scale shaking table tests proved that the M-O method predicted resultant force was quite realistic when 'enough' outward displacement of the wall occurred, leading to the development of a Coulomb sliding surface in the retained soil. However, frequently in practice (basement and braced walls, bridge abutments) the imposed kinematic constraints do not lead to the development of limit-equilibrium conditions, and thereby increased dynamic earth pressures are generated. Elastic solutions were developed like Wood's solution [33] which for a rigid wall fixed at its base lead to pseudo-static earth pressures hereby 2.5 times higher than M-O.

The two groups of methods mentioned above (limit-equilibrium and elastic) seem to cover the two extreme cases. The limit-equilibrium methods assume rigid plastic behaviour, while the elastic methods regard the soil as a visco-elastic continuum. Efforts to bridge the gap between the above extremes have been reported by Whitman and his co-workers [1,18]. Their analyses combine wave propagation in a visco-elastic continuum with concentrated plastic deformation on a failure surface. Based on this categorization, many codes estimate the dynamic earth pressures according to the potential of the wall to deform. For example, for the seismic analysis of bridge abutments, the Regulatory Guide E39/93 [23] proposes three different cases for the calculation of the dynamic earth pressures depending on the ratio between the expected (or allowable) displacement at the top of the wall U to its height H (see Fig. 2). As it is possible for the wall-soil system to develop material (or even geometric) non-linearities, it is difficult to distinguish the limits between the three cases. The main reason is that the displacement U cannot be predefined. It is obvious though that the minimum dynamic earth pressures are predicted in the case of flexible walls ($U/H > 0.10\%$), while the dynamic pressures are 2.5 times higher in the case of perfectly rigid and immovable walls ($U/H < 0.05\%$). For intermediate cases the dynamic earth pressures are somewhere between the maximum and minimum values.

More recently, Veletsos and Younan [31] proved that the high dynamic earth pressures proposed by elastic methods decrease substantially if the structural flexibility of the wall and the rotational compliance at its base are taken into account. Fig. 3 [22] highlights the beneficial effect of wall and base flexibility in not only reducing the resultant force to values similar to those of M-O, but also lowering its height of application to values of about 1/3 of H [31].

Several other phenomena, not reflected in the analyses of Fig. 3, may also lead to further decreasing of both ΔP_{AE} and h_{AE}. Two examples (in Fig. 4 and Fig. 5) illustrate graphically this beneficial effect.

Fig. 4 [22] studies the effect of elastic non-homogeneity of the retained soil. Such a non-homogeneity reflects in a very simple way not only the unavoidably reduced soil stiffness under the small confining pressures prevailing near the top, but also two more strong-shaking effects:

- the softening of the soil due to large shearing deformations
- the non-linear wall–soil interface behaviour, including separation and slippage

Apparently, the soil pressures along the top half of the wall decrease substantially, and in the case of a flexible wall they become insignificant.

Fig. 5 addresses a number of factors affecting the response, including:

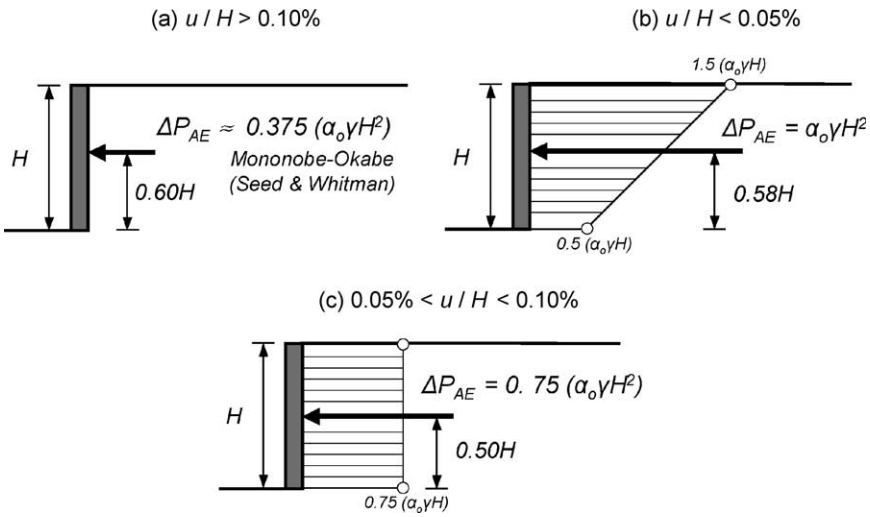

Fig. 2. Typical dynamic pressure distributions proposed by seismic bridge codes for seismic analysis of abutments (e.g. the Greek Regulatory Guide E39/93). Situations (a) and (b) correspond to the two extreme cases: (a) of yielding wall supporting elasto-plastic soil in limit equilibrium, and (b) of undeformable and non-yielding wall supporting purely elastic soil. Case (c) is an intermediate stage.

- the presence of an underlying soil layer, supporting the wall and the backfill
- the inelastic material behaviour of both the retained and the supporting soil
- the frequency content of the base excitation.

The former allows elastic translation and rotation to occur at the base, both of which have a distinct beneficial effect on wall pressures. (In addition, wave propagation through this layer may change the character of the motion experienced by the top 'backfill' soil.) Inelastic material behaviour of the soil would in most cases further reduce the dynamic wall pressure to values which may only be a fraction of M-O. Finally, the effect of the frequency content of base excitation is examined by using three accelerograms (Fig. 6): two idealized Ricker wavelets [25] with central frequencies $f_0 = 4$ Hz (high frequency) and $f_0 = 2$ Hz (medium frequency), and the moderately low-frequency Aegion rock outcrop accelerogram [2]. Evidently, a high frequency excitation (such as, for example, the ground motions in downtown Athens during the 1999 earthquake) would lead to pressures substantially lower than M-O.

While the above are merely realistic examples, not covering all possible cases, their trend is clear: soil action on the wall tends to decrease as the *degree of realism* in the analysis increases to include such effects as structural flexibility, foundation soil deformability, material soil yielding, and soil-wall separation and sliding.

Hence it is quite conceivable that in many cases of walls subjected to earthquakes, the total shear force and overturning moment acting at the base of the wall will be smaller

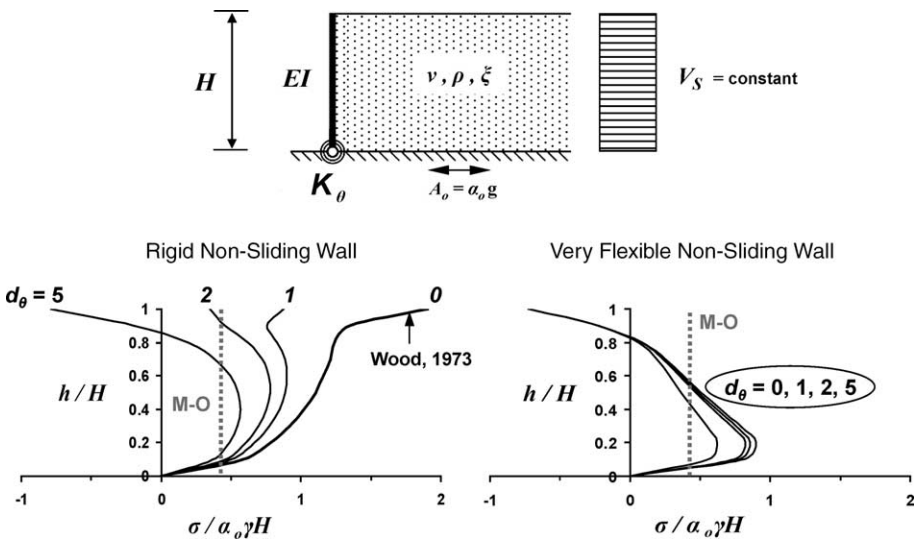

Fig. 3. Elastic dynamic earth-pressure distribution of a pseudo-statically excited one-layer system for a non-sliding retaining wall. The cases of rigid and very flexible wall are examined for various values of relative rotational flexibility of its base ($d_\theta = \rho V_S^2 H^2 / K_\theta$), after Veletsos & Younan [31] and Psarropoulos et al. [22] ($\gamma = \rho g$ the unit weight of the soil).

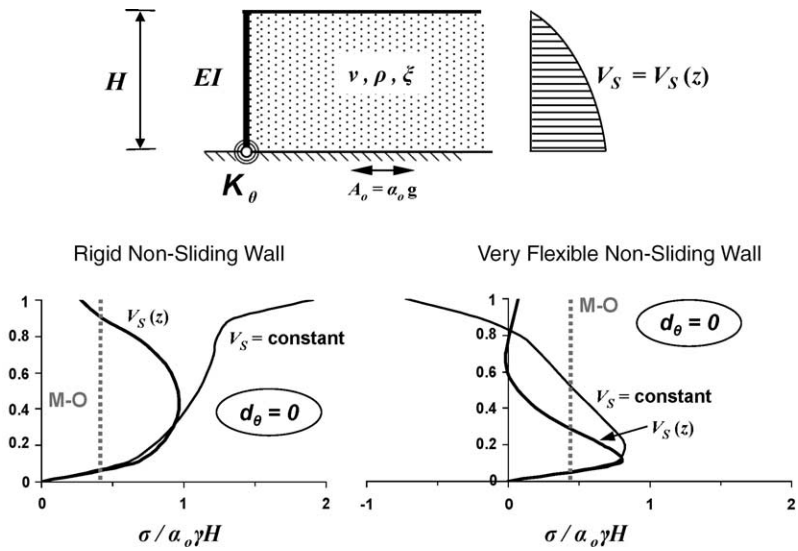

Fig. 4. Effect of soil non-homogeneity on the elastic dynamic earth-pressure distribution for a fixed-based wall ($d_\theta = 0$). Comparison with the corresponding curves for the homogeneous soil from Fig. 3, after Klonaris [11] and Psarropoulos et al. [22].

than those computed with M-O for the same base acceleration. However, M-O has been used (at least in the past) with acceleration levels rarely exceeding 0.15 g. How then could such walls survive amplitudes of (effective) acceleration of up to 0.45 g—i.e. three times higher than design seismic coefficient ? The answer in structural engineer's terms: by being very 'ductile'.

The high 'ductility' capacity in LRC type of walls (as well as in gravity walls, in general) stems not from the ductility of its structural component (the RC), but from the wall-base-supporting-soil interface. The 'plastic hinge' at this location takes of course the form of interface sliding. Richards and Elms [24] were the first to propose that every time the base acceleration is such that the shear force tending to develop exceeds the frictional capacity of the interface (i.e. wherever the instantaneous Factor of Safety [FS] is below unity) sliding takes place. The larger force will simply not materialize, with the penalty being the development of permanent slippage, Δ. It turns out that even for FS as low as 1/3, Δ will in most earthquake cases be not

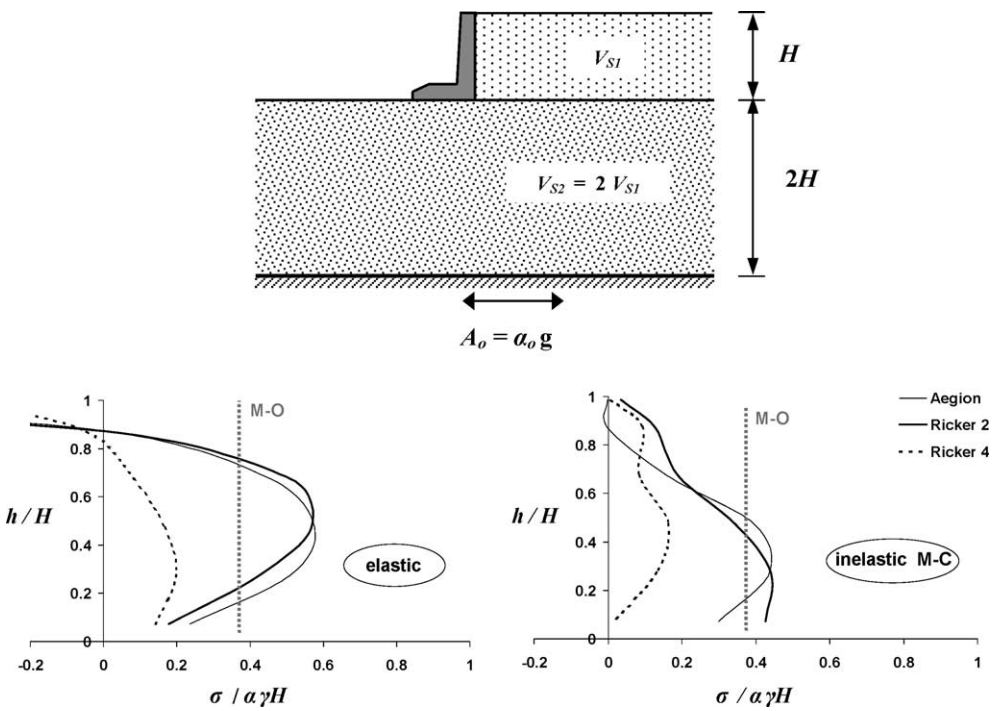

Fig. 5. The two-layer model subjected to three seismic base motions with maximum acceleration $A_o = 0.40$ g. Distribution of dynamic earth-pressures in case of: (a) elastic and (b) elasto-plastic Mohr–Coulomb soil behaviour. $A(= \alpha g)$ is the peak acceleration at the mid-depth of the retained soil.

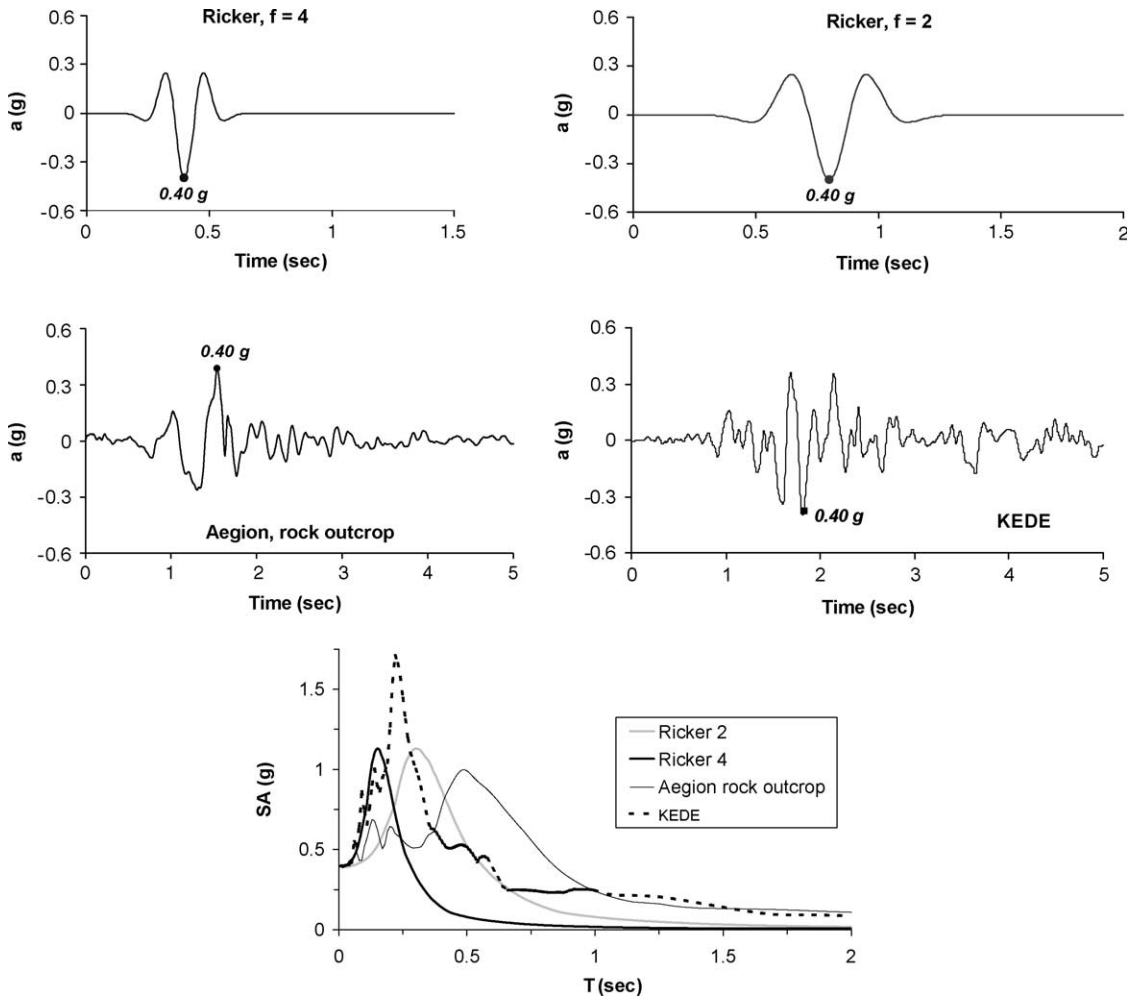

Fig. 6. Idealized and recorded acceleration time histories, normalized to PGA = 0.40 g, utilized in the paper with their response spectra. Two Ricker pulses and the Aegion record are used in the numerical analyses, while the KEDE record is used only in the analyses of the Kerameikos case history.

more that about 10 cm—hardly a detrimental displacement in a very strong event. Moreover, Δ is almost inversely proportional to f_E^2, the square of the dominant frequency of excitation. An $f_E > 3$ Hz would lead to less than 5 cm of permanent displacement with an instantaneous minimum FS $\approx$ 1/4.

Combining all the above arguments leads to the conclusion that even when designed with the very small

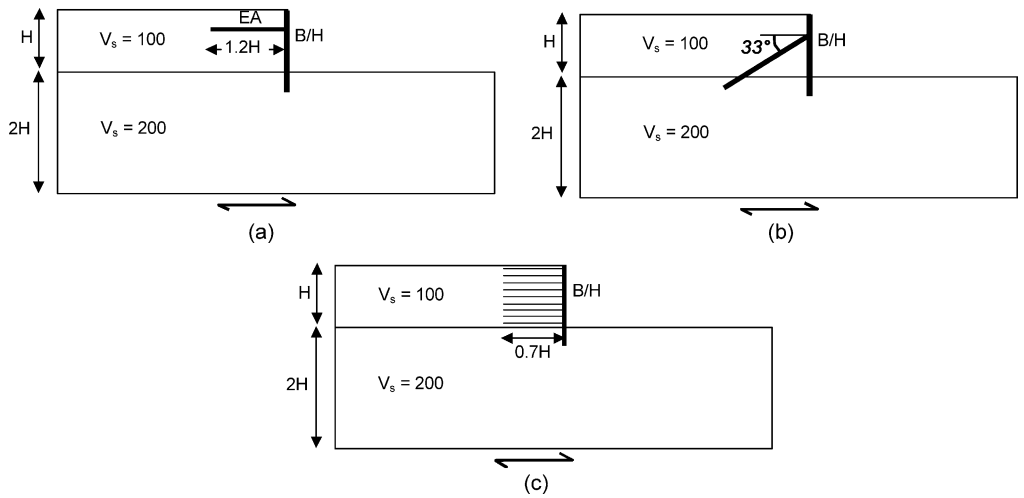

Fig. 7. The three different flexible walls considered in the study: (a) prestressed-anchored pile (PAP) wall with horizontal anchors, (b) PAP wall with inclined anchors, and (c) reinforced-soil (RS) wall.

horizontal acceleration of the past, semi-gravity LRC walls can easily survive strong shaking.

5. Walls with structural flexibility and structural constraints

To shed some light on the dynamic performance of retaining walls that combine structural flexibility with structural constraints, a series of numerical analyses are conducted for the systems sketched in Fig. 7:

(a) a Prestressed-Anchor Piled (PAP) wall with horizontal anchor,
(b) a Prestressed-Anchor Piled (PAP) wall with inclined anchor, and
(c) a Reinforced-Soil (RS) type retaining wall.

In all three cases, the wall height is $H = 10$ m, and is founded on a deformable soil layer of thickness $2H$. The upper soil layer has a shear wave velocity $V_S = 100$ m/s, while for the bottom soil layer $V_S = 200$ m/s. For the first two cases, the anchor has a total length of $1.2H$, half of it being grouted, and fixed to the wall at $0.7H$. In the second case the anchor is inclined with an angle of 33° to the horizontal. This inclination is rather steep when compared to the usual ones that range from 10 to 20°. However, special cases requiring at least as steep inclinations also exist in life. The 33° inclination is a reasonable value to obtain an upper bound solution for the effect of anchor inclination.

For the first two cases the wall rigidity was parametrically examined, by analysing, a lower bound of $B/H = 0.03$, where B is the equivalent uniform thickness of the wall, and an upper bound of $B/H = 0.11$. The first case

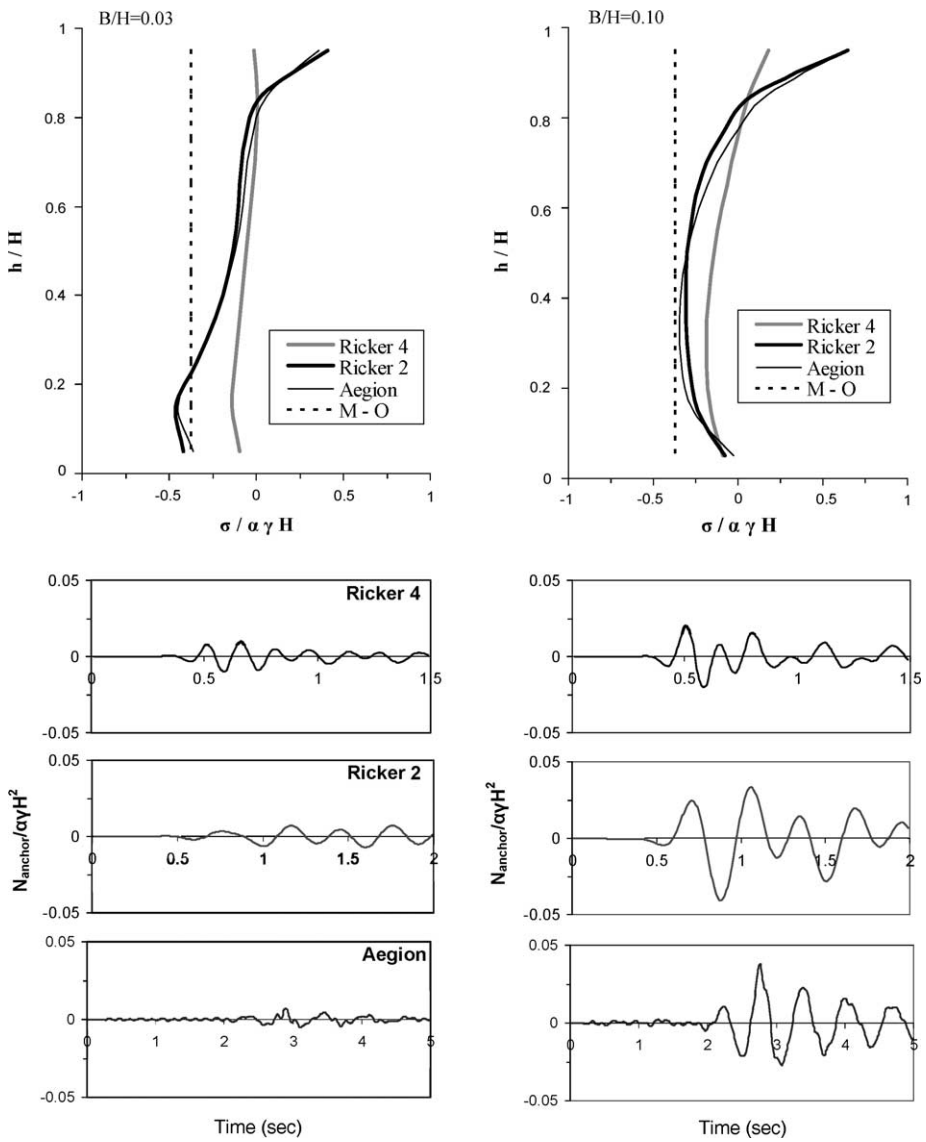

Fig. 8. PAP wall: effect of the frequency content of seismic excitation and of rigidity of the wall on the dynamic wall pressures and anchor forces, for the case of linear elastic soil and horizontal anchors.

would be equivalent to a Berlin-type piled with 0.6 m diameter piles spaced horizontally at 1.0 m, or to a diaphragm wall; the second of a secant piled wall with 1.2 m diameter piles spaced at 1.0 m. The flexibility of the anchoring cable was also parametrically investigated. The most rigid anchor has $EA = 500$ MN; the flexible: $EA = 16$ MN, where E is the steel modulus of elasticity and A the anchor cross-sectional area. In the third case, soil reinforcement replaced the anchors. The nails are spaced vertically at 1 m, their length is $0.7H$, and the wall consists of a thin rigid facing.

For all three cases, elastic and inelastic analyses are conducted. For the latter Mohr–Coulomb failure criterion is utilized, with friction angle $\varphi = 35°$, dilatancy angle $\psi = 5°$, and cohesion $c = 2$ kPa—parameters characteristic of (non-clean) sandy materials often used as backfill.

The results of the analyses are presented mainly in the form of dimensionless graphs. Normalized dynamic wall pressures $\sigma/\alpha\gamma H$ and dynamic anchor forces $N_{\text{anchor}}/\alpha\gamma H^2$ (where α is the free-field acceleration, in units of g at $H/2$ from the bottom of the wall) are compared with the M-O. All analyses implicitly assume that the anchoring system possesses a substantial factor of safety against pullout.

5.1. Effect of excitation frequency content and of wall rigidity

Fig. 8 depicts the distributions along the wall of dynamic pressures and anchor forces for the cases of a very flexible ($H/B = 0.03$), and a relatively rigid ($H/B = 0.11$) wall, assuming elastic soil behaviour. It is evident that the high-frequency Ricker 4 wavelet causes smaller pressures and anchor forces than the longer-period Ricker 2 and Aegion, in both wall cases. The dynamic pressures are larger for the rigid wall as the flexible wall tends to follow more closely the deformation of the ground. For the rigid wall the anchor forces are higher for Ricker 2 and Aegion than for Ricker 4; such is not exactly the case for the flexible wall. In all cases, however, the dynamic wall pressures are much lower than those predicted with M-O (dashed line).

5.2. Effect of anchor inclination

To examine the effect of anchor inclination both rigid and flexible anchors are considered. For the case of horizontal anchors, contrary to the rigidity of the wall, which has been shown to play an important role, the anchor stiffness is not a crucial factor. As shown in Fig. 9, as the anchors become inclined the anchor flexibility becomes important. Both dynamic pressures and anchor forces increase with anchor inclination, and anchor stiffness. Observe that with inclined anchors the dynamic pressures build-up at a height of about $0.7H$, where the anchor is fixed to the wall. The mechanism producing this increase in wall pressures and anchor forces is as follows: when the anchor is horizontal, given the flexibility of the wall (which is flexible even for $H/B = 0.11$), the wall tends to deform in conformity with the nearby free-field soil.

Hence, the anchor is not undergoing extension: the anchor grout moves dynamically in near unison with the wall. However, when the anchor is inclined, its tip is located deeper than its connection with the wall, leading to differential and out-of-phase movement of its two edges. Since the top of the wall (and the soil layer beneath it) has the tendency to move more than its bottom, the anchor undergoes dynamic extension, which also generates high wall pressures. As illustrated in Fig. 10, due to the tendency of the top of the wall (and the soil layer beneath it) to move outwards more than its bottom, the anchor undergoes dynamic tension, which also generates high wall pressures.

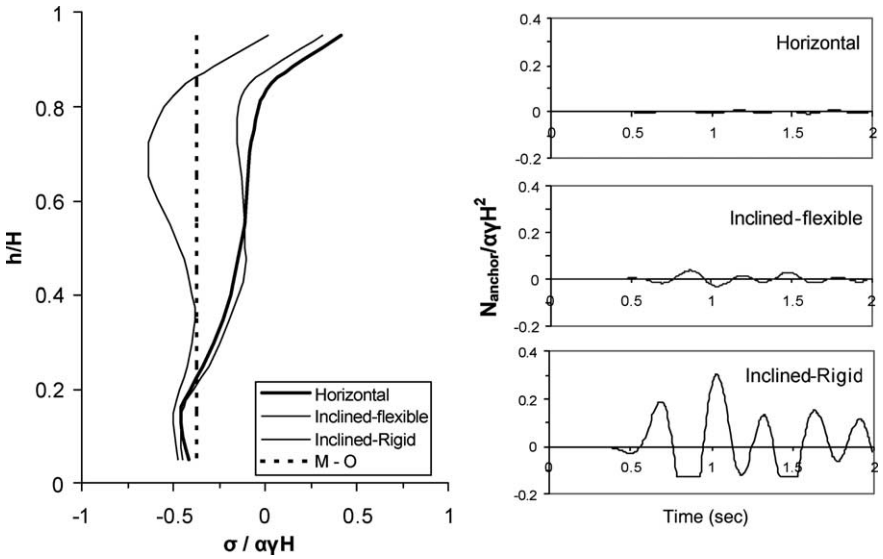

Fig. 9. PAP wall: effect of anchor inclination and stiffness on dynamic wall pressures and anchor forces, for the case of linear elastic soil, and Ricker 2 seismic excitation.

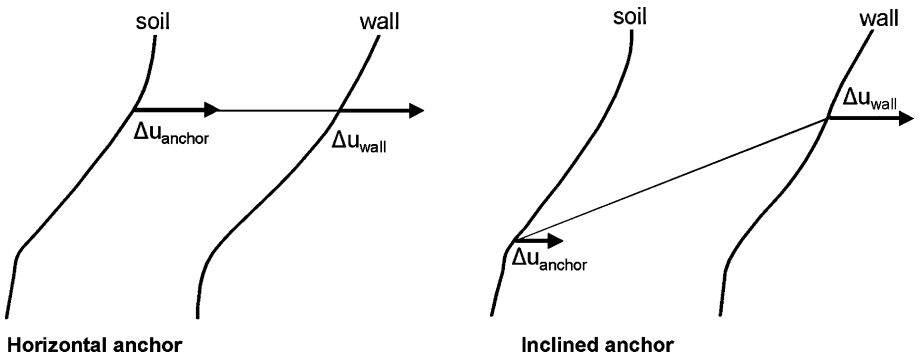

Fig. 10. Displacements of the wall compared with the displacements of the soil at a vertical section passing from the end of the anchor. Contrary to the horizontal anchor, which is not dynamically stressed, the inclined one is tensed since the upper part of the wall tends to move outwards more than its bottom, where the anchor is attached.

Obviously, this anchor tensile force increases with increasing stiffness *EA*, and hence the dynamic wall pressures also increase. Again, with the exception of the rigid inclined anchor, wall pressures are smaller than M-O.

5.3. Effect of inelastic soil behaviour

As shown in Fig. 11, in contrast to the unpropped retaining walls referred in Fig. 5 the dynamic pressures increase in the pressure of soil inelasticity for the case of wall with horizontal anchor. But now the pressures tend to decrease with increasing anchor stiffness. The anchor forces also increase dramatically with soil inelasticity. Notice that the anchor forces are similar with flexible and with rigid anchors. Furthermore, residual forces are observed in the anchors. The mechanism in this case is different from the one in the previous case. With a rigid anchor, the failure of soil elements behind the wall is of more limited extent, than with a flexible anchor. So, increasing anchor flexibility the soil fails easier a Coulomb sliding interface forms, the wedge tends to slide, and thus the holding anchor undertakes a heavy load. Naturally, such deformation is irreversible residual forces on the wall.

The situation is different with an inclined anchor (Fig. 12). With both the flexible and the rigid anchor, the wall pressures decrease with soil inelasticity. This decrease is higher with the flexible anchor. At the same time, the dynamic anchor forces with rigid anchor tend to decrease slightly, while they tend to increase with flexible anchor. Again, residual anchor forces develop. A possible explanation of this difference is as follows: with soil behaving non-linearly the kinematic effect is reduced since the differences between the displacements of the two edges of the anchor tend to be smoothened out. In support of this mechanism, see that the anchor forces, tend to decrease slightly with soil non-linearity. The increased negative anchor forces for the flexible anchor case are not important, since they mean unloading of the anchor.

With soil non-linearity being accounted for, the dynamic wall pressures are invariably smaller than the M-O pressures, even with a rigid inclined anchor.

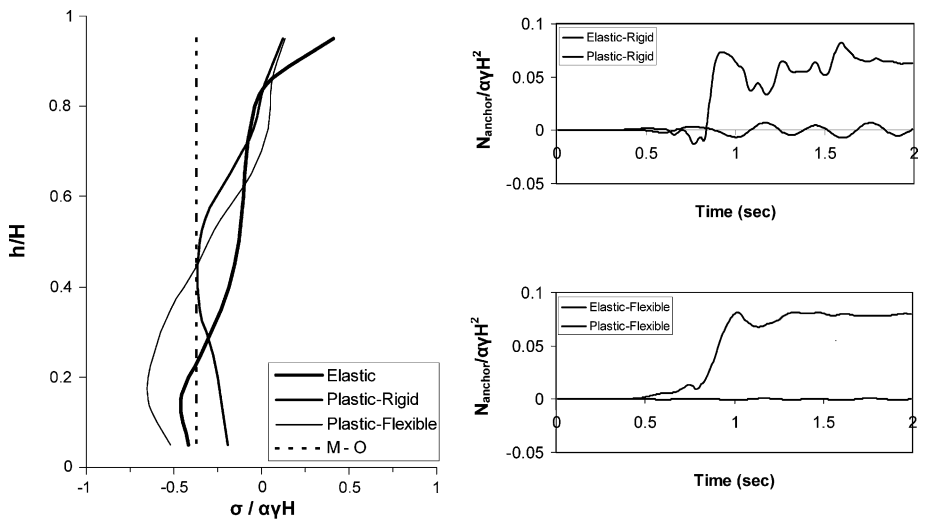

Fig. 11. PAP wall: effect of soil inelasticity on dynamic wall pressures and anchor forces, for the case of horizontal anchor, and Ricker 2 seismic excitation.

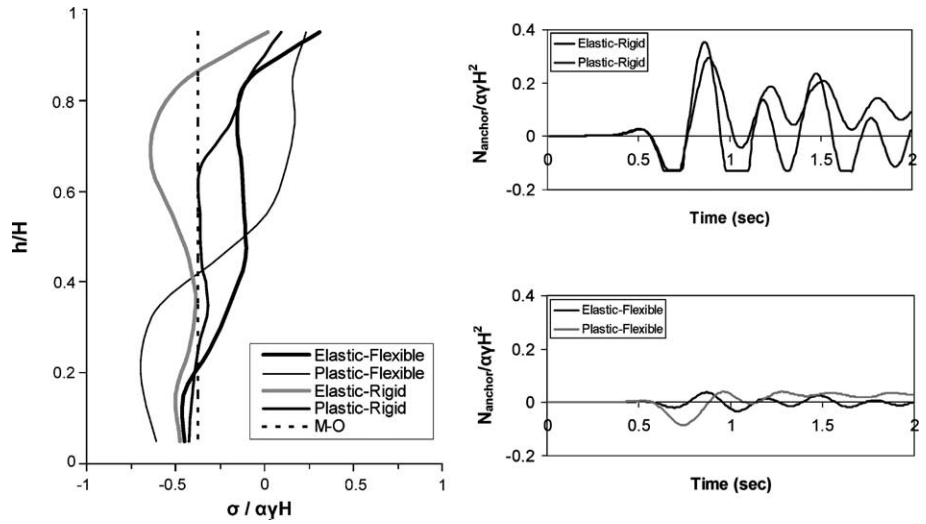

Fig. 12. PAP wall: effect of soil inelasticity on dynamic wall pressures and anchor forces, for the case of an inclined anchor, and Ricker 2 seismic excitation.

6. The 'Kerameikos station' case history

A case history of excellent behaviour of a retaining system subjected to short-duration moderately strong excitation is the Kerameikos metro station in Athens, Greece. The station of Kerameikos had been abandoned for non-technical reasons at the end of 1996, and thus at the time of the 1999 M_S 5.9 Athens (Parnitha) earthquake only the 'temporary' retaining walls had been constructed and remained in place.

As shown in Fig. 13, the excavation had reached 23 m, with the retaining system comprising cast-in-place reinforced-concrete piles of 0.8 m diameter, spaced at 1.8 m. The vertical faces had been covered with 15 cm thick shotcrete. Each pile was tied back with 5–7 slightly inclined (15°) anchors, having a total length varying from 12 to 24 m, and a bonded length from 6 to 13 m. The soil profile comprises 5–7 m of alluvial clayey sand, followed by a soft weathered rock, called locally 'Athenian Schist', exhibiting a stiff-soil-type behaviour, with a degree of heterogeneity. The soil properties used in our analyses are the following:

- Alluvial layer (0–7 m): $\gamma = 20.5$ kN/m^3, $\varphi = 30°$, $c = 0$ kPa, $E = 20$ MPa.
- Underlying layer (7–30 m): $\gamma = 23$ kN/m^3, $\varphi = 28°$, $c = 15$ kPa, $E = 100$ MPa.

The retaining structure had not been designed against earthquake, since it was meant to be only temporary. However, although subjected to PGA levels of at least 0.40 g, no damage was reported after the main shock and the aftershocks. A few minor cracks were 'discovered' in the shotcrete, but it is not clear whether they were due to the shaking or existed before the earthquake.

To verify this exceptional behaviour we conducted two-dimensional finite-element analyses. The potential soil non-linearity is taken into account by utilizing equivalent soil properties obtained by one-dimensional equivalent linear

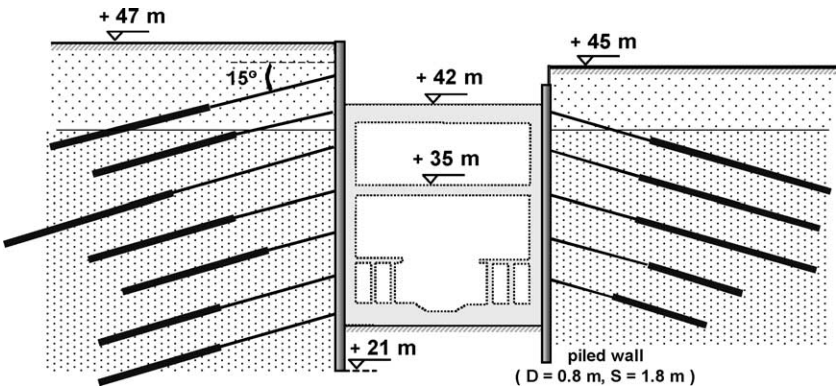

Fig. 13. Typical cross-section of the Kerameikos station. The inner structure (dotted lines) was never built. The 'temporary' support of the excavation was subjected to a high-frequency PGA ≈ 0.50 g top motion during the 1999 Athens (Parnitha) earthquake. No damage was observed, although the support had not been designed against earthquake.

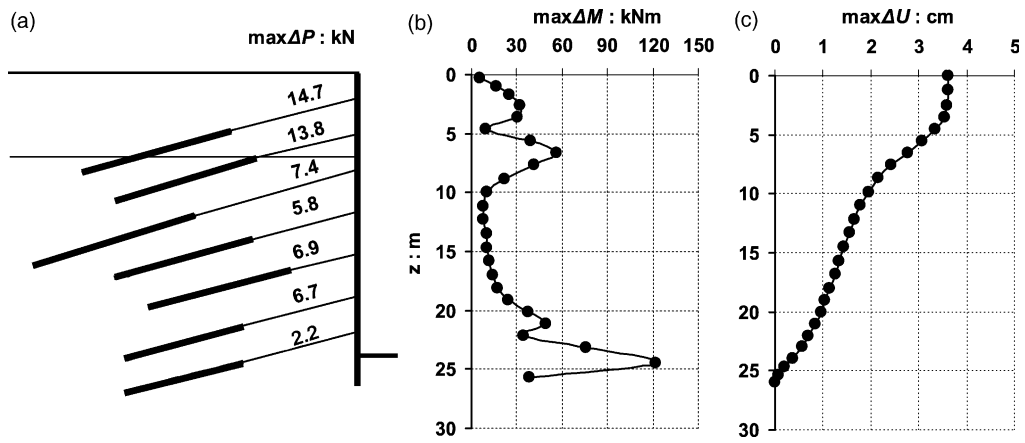

Fig. 14. Numerical results for the left-hand-side wall of the Kerameikos station subjected to the Athens (Parnitha) earthquake: (a) peak values of axial force, ΔP, on each anchor, (b) distribution with depth of the peak bending moment, ΔM, in each pile, and (c) distribution with depth of the peak horizontal piled wall displacement, ΔU.

analyses. The rock-outcrop motion of KEDE record (see Fig. 6) was used as base excitation, since the station was located at a distance less than 1 km away [6].

Our numerical results for the left-hand-side wall of the station are plotted in Fig. 14. The peak values of axial force on each anchor, the distribution with depth of the peak bending moment in each pile, and the distribution with depth of the peak horizontal piled wall displacement are shown.

First, it is mentioned that computed PGA value at the crest of the wall reached 0.55 g and the free field (backfill) 0.50 g, compared to the 0.40 g of the base excitation.

The bending moments in each pile are found to be very small (max $\Delta M \leq 120$ kNm) for a $D = 0.8$ m reinforced-concrete wall. The local peaks at depth of about 7 m (max $\Delta M \approx 60$ kNm) is obviously associated with the interface between the two soil layers of different stiffness ('kinematic' effect, see Gazetas and Mylonakis [4]).

The values of the anchor forces, ΔP, are only a small fraction (not more than about 4%) of the static prestress forces (of the order of 400 kN). Such low values are a consequence of negligible soil non-linearities behind the wall and, thereby, in-phase movement of the points along an anchor—as already addressed in the preceding sections.

Finally, the computed peak values of seismic displacements (less than about 3.5 cm) are consistent with the excellent uncracked performance of the shotcrete face.

With the retaining structure being subjected to such high PGAs, one might have expected that damage would be serious. In reality, no damage was observed. The wall, thanks to its inherent flexibility relative to the stiff soils, follows the ground motion without being substantially stressed. Although the nearly horizontal anchors play a very significant role statically, they simply follow the movement of the ground under the specific dynamic excitation.

Note that the high frequency content of the motion is another key factor for the success of the Kerameikos retaining wall. Had the excitation been richer in long periods, the structure might not have performed so well.

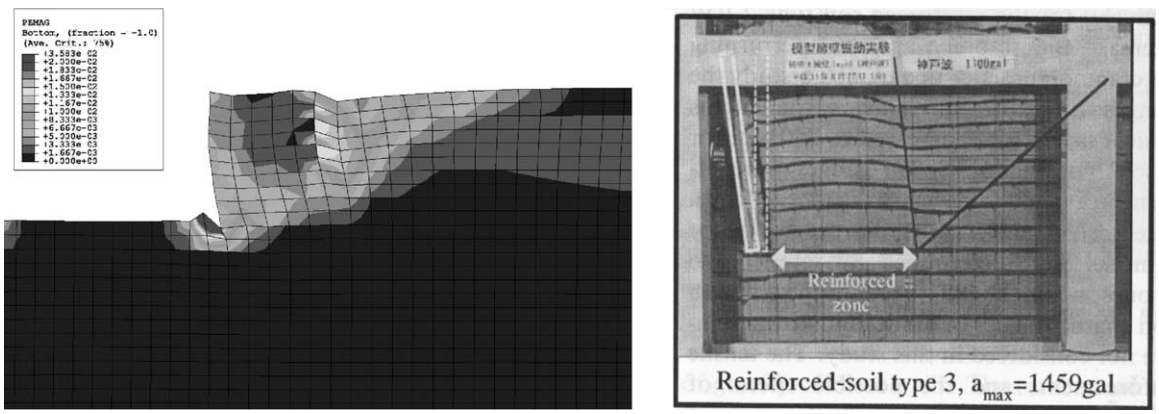

Fig. 15. Reinforced-soil wall: quantitative comparison of finite element analysis and centrifuge experiments for plastic deformation magnitude. (Experiment by Koseki [13].)

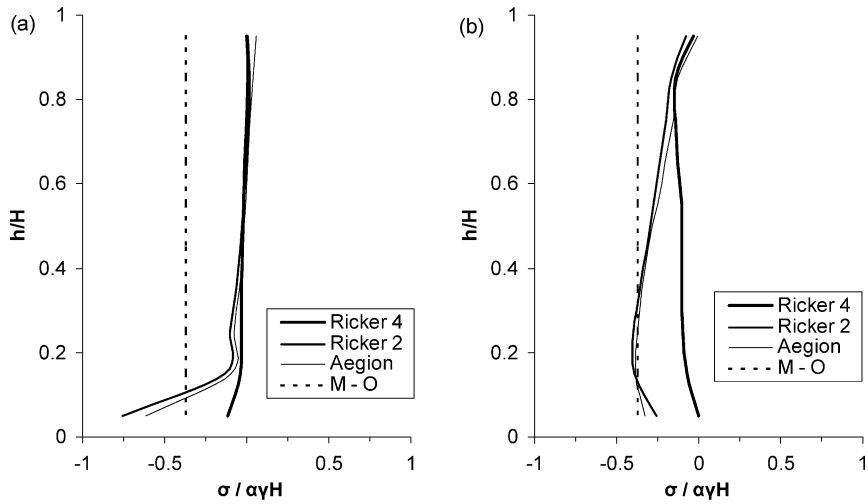

Fig. 16. RS wall: dynamic wall pressures for (a) linear elastic soil, and (b) inelastic M-C soil.

7. Dynamic behaviour of the reinforced-soil (RS) retaining wall

In Fig. 15 a snapshot of the magnitude of plastic deformation in the finite element model is quantitatively compared with experimental results [13]. The reinforced-soil zone tends to move as a rigid block, with the failure of the soil mainly taking place behind it. Notice the similarity of the failure mechanisms captured with the finite element analysis and actually observed in the experiment. Fig. 16 compares the dynamic wall pressures developed by all excitations for elastic and inelastic soil. The pressures are practically insignificant as long as the soil behaves linearly. However, when the soil behind the reinforced zone starts failing, wall pressures increase significantly. For the Ricker 4 excitation this increase is distributed along the whole height of the wall; for Ricker 2 and Aegion the pressures tend to reach a nearby triangular distribution. In all cases, the dynamic wall pressures remain lower than the M-O solution. As shown in Fig. 17, the dynamic forces in the 'anchor' (passive reinforcement or nails in this case) increase dramatically with soil inelasticity, exhibiting residual values as well. It is important to observe that the bottom soil nail attracts the greatest dynamic load. To explore the role of vertical acceleration, the above analysis was repeated with simultaneous horizontal and vertical excitation. Two scenarios were analysed:

(a) Ricker 2 (+) horizontal acceleration and Ricker5 (±) vertical acceleration, and
(b) Ricker 2 (−) horizontal acceleration and Ricker5 (±) vertical acceleration.

As depicted in Fig. 18, the effect of vertical acceleration on the dynamic wall pressures is apparently even more negligible than the pseudo-static M-O solution despite the severe assumption of simultaneous occurrence and equal amplitude of the horizontal and vertical peaks.

All non-linear analyses were performed with 0.40 g of base ground acceleration. This acceleration is amplified to almost 0.70 g (at $H/2$, i.e. the middle of the backfill) for the Ricker 2 excitation. The amplification is a little higher for Aegion and a little lower for Ricker 4. Evidently, this RS wall model was subjected to PGAs similar to those experienced by similar walls during the Kobe and the Chi-Chi earthquakes. Our finite element analysis model does not

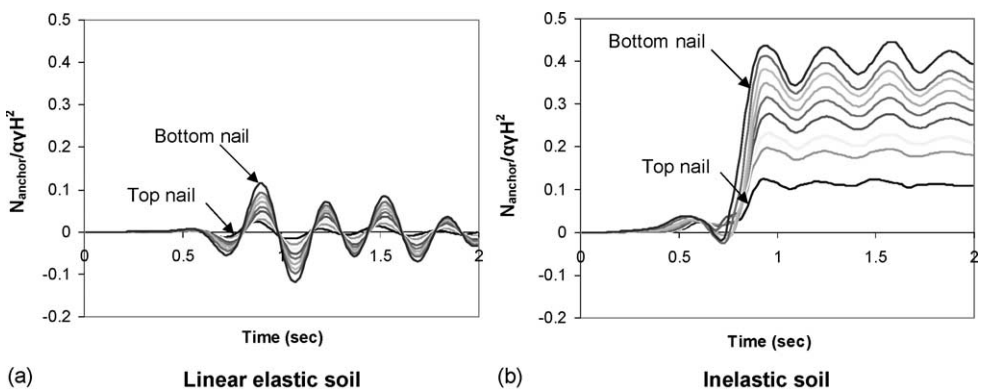

Fig. 17. RS wall: effect of soil inelasticity on dynamic forces in the reinforcing bars. Ricker 2 seismic excitation.

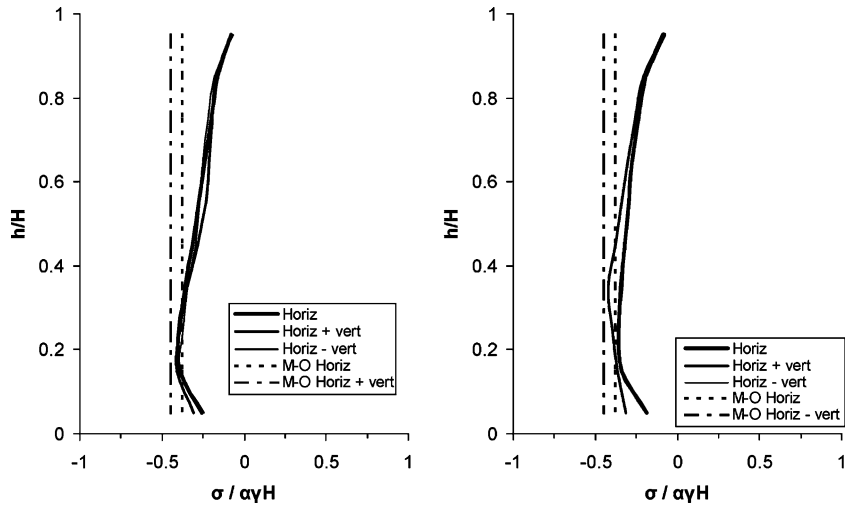

Fig. 18. RS wall: effect of vertical acceleration on dynamic wall pressures for simultaneous excitation with: (a) + Ricker 2 horizontal acceleration and ± Ricker 5 vertical acceleration, and (b) − Ricker 2 horizontal acceleration and ± Ricker 5 vertical acceleration. The effect of vertical acceleration is evidently negligible.

predict any dramatic deformation that could be interpreted as 'practical failure'. The permanent horizontal displacements reach 6 cm for the Ricker 2 and the Aegion excitations, while being less than 2 cm for the Ricker 4 excitation. The modelling is fairly realistic for walls with full height rigid facings, such as the ones of Kobe. For the mentioned case of Taiwan, where the walls were not equipped with rigid facings, things are a little different. As we saw, with the longer period excitations the pressures tend to accumulate at the base of the wall. Also, the anchor forces are much higher for the bottom anchors than for the top ones. So, at the bottom of the wall the facing could locally fail, leading to a failure of the same type as in Chi-Chi.

8. Conclusions

The key conclusions of the study are as follows:

(a) L-shaped reinforced-concrete walls will in many cases be subjected to dynamic pressures smaller than M-O. This is especially true with high frequency excitation, and when sliding and separation between wall and soil takes place. Exceptions to this general rule exist, such as when the backfill characteristics are such that significant soil amplification of the motion may take place. These exceptions, which have not been addressed in the paper, are rather infrequent and they do not change our general thesis. In any case, even if soil pressures computed with realistically high accelerations were to exceed the M-O pressures computed with conventionally low accelerations, these retaining systems possess sufficient 'ductility' capacity, in the form of unhindered slippage at their base, thanks to which they can survive even a strong event with minor damage.

(b) Prestressed-anchor pile or diaphragm walls, as well as reinforced-soil walls possess enough flexibility to lead to earth pressures that in most cases are smaller than M-O, especially along the upper half of the wall. The maximum (and the residual) axial forces in the anchors of the reinforcing strips are of small or moderate magnitude even under very strong seismic shaking. The possible exceptions refer to:
   (i) the case of strongly inclined and rigid anchors, which produce higher wall pressure and attract larger forces than those computed with M-O; and
   (ii) the case of thinly reinforced RS walls, the lowest strips of which attract high axial forces, risking pull-out failure.

(c) Even a severe simultaneous vertical acceleration does not appear to have any measurable effect on either the soil pressures against the walls, or on the sliding displacements at the base. They could safely be ignored in most design.

The results of this study are consistent with the good performance of such walls during earthquakes. The response of the Kerameikos metro station during 1999 Athens (Parnitha) earthquake, which was analysed in the paper, is not exception to the rule.

References

[1] Al-Homoud AS, Whitman RV. Seismic analysis and design of rigid bridge abutments considering rotation and sliding incorporating nonlinear soil behaviour. Soil Dyn Earthquake Engng 1999;18:247–77.
[2] Gazetas G. Soil dynamics and earthquake engineering—case histories. Athens, Greece: Symeon; 1996. in Greek.
[3] Gazetas G, Dakoulas P, Dennehy K. Empirical seismic design method for waterfront anchored sheetpile walls. Des Perform Earth Retaining Struct, ASCE 1990;232–50.

[4] Gazetas G, Mylonakis G. Seismic soil–structure interaction: new evidence and emerging issues. Soil Dynamics III, ASCE, Specialty Geotechnical Conference, Seattle 1998;2:1119–74.
[5] Gazetas G, Protopapa E, Gerolymos N. The response of two Athens metro stations in the Parnitha earthquake: records and analysis. Proceedings of the Fourth Hellenic Conference on Geotechnical and Geoenvironmental Engineering, Athens, 2001, vol. 2.; 2001. p. 131–38, in Greek.
[6] Gazetas G. Analytical and experimental estimation of the ground motions in the meizoseismal region of the Athens 7-9-99 earthquake. Research Report to OASP; 2001: vol. 1–3.
[7] Ghalandarzadech A, Orita T, Towata I, Yun F. Shaking table tests on seismic deformation of gravity quay walls. Soils Found, Spec Issue 1998;94–114.
[8] Inagaki H, Iai S, Sugano T, Yamazaki H, Inatomi T. Performance of Caisson Type Quay Walls at Kobe Port. Soils and Foundations. Special Issue on the Geotechnical Aspects of the January 17 1995 Hyogoken-Nambu Earthquake, 1996; 119–36.
[9] Ishihara K. Geotechnical aspects of the 1995 Kobe earthquake. Terzaghi Oration, Proceedings of the 14th ICSMFE, Hamburg; 1997.
[10] Kitajima S, Uwabe T. Analysis of Seismic Damage in Anchored Sheet-Piling Bulkheads. Report of the Japanese Port and Harbor Research Institute, 1979; 18, 67–130 (in Japanese), summarized in Ebeling and Morrison, 1993.
[11] Klonaris G. Dynamic analysis of pressures and deformations of retaining structures, Diploma Thesis. National Technical University of Athens, 1999 (in Greek).
[12] Koseki J, Tatsuoka F, Munaf Y, Tateyama M, Kojima K. A modified procedure to evaluate active earth pressure at high seismic loads. Soils Foundations, Special Issue on Geotechnical Aspects of the January 17 1995 Hyogoken-Nambu Earthquake, vol. 2.; 1998. p. 209–16.
[13] Koseki J. Seismic performance of retaining walls—case histories and model tests. Proceedings of the Fourth Forum on Implications of Recent Earthquakes on Seismic Risk, Japan: Tokyo Institute of Technology; 2002. p. 95–107.
[14] Lew M, Simantob E, Hudson ME. Performance of shored earth retaining systems during the January 17, 1994, Northridge earthquake. Proceedings of the Third International Conference on Recent Advances in Geotechnical Earthquake Engineering and Soil Dynamics, St Louis, Missouri, vol. 3.; 1995.
[15] Ling HI, Leshchinsky D, Chou N. Post-earthquake investigation on several geosynthetic-reinforced soil retaining walls and slopes during the Ji-Ji earthquake of Taiwan. Soil Dyn Earthquake Engng 2001;21: 297–313.
[16] Mitchel JK (Coordinator). Performance of improved ground and earth structures. The 1999 Kocaeli Earthquake Reconnaissance Report. EERI, 2000; 16A: 191–225.
[17] Mononobe N, Matsuo H. On the determination of earth pressures during earthquakes. Proceedings of the World Engineering Congress, Tokyo, vol. 9.; 1929. p. 177–85.
[18] Nadim F, Whitman RV. Seismically induced movement of retaining walls. J Geotech Engng, ASCE 1983;109(7):915–31.
[19] Okabe S. General theory of earth pressures. J Jpn Soc Civil Engng 1926;12(1).
[20] Pamuk A, Kalkan E, Ling HI. Structural and geotechnical impact of surface rupture in highway structures. Proceedings of the 11th ICSDEE and Third EGE, vol. 1.; 2004. p. 294–301.
[21] PIANC, Seismic design guidelines for port structures. Rotterdam: Balkema; 2000.
[22] Psarropoulos P, Klonaris G, Gazetas G. Seismic response of retaining walls. Proceedings of the Fourth Hellenic Conference on Geotechnical and Geoenvironmental Engineering, vol. 2.; 2001. p. 377–85, in greek.
[23] Regulatory Guide E39/93 for the seismic analysis of bridges (Ministry of Public Works). Bulletin of Greek Technical Chamber, No. 2040; 1998.
[24] Richards R, Elms DG. Seismic behavior of gravity retaining walls. J Geotech Engng Div, ASCE 1979;105:449–64.
[25] Ricker N. The form and laws of propagation of seismic wavelets. Geophysics 1960;18:40.
[26] Scott RF. Earthquake-induced pressures on retaining walls. Proceedings of the Fifth World Conference on Earthquake Engineering, vol. 2.; 1973. p. 1611–20.
[27] Seed HB, Whitman RV. Design of earth retaining structures for dynamic loads. Proceedings of the Specialty Conference on Lateral Stresses in the Ground and Design of Earth Retaining Structures, ASCE; 1970. p. 103–47.
[28] Tatsuoka F, Tateyama M, Koseki J. Performance of soil retaining walls for railway embankments. Soils and Foundations, Special Issue on Geotechnical Aspects of the January 17 1995 Hyogoken-Nanbu Earthquake, vol. 1.; 1996. p. 311–24.
[29] Tatsuoka F, Koseki J, Tateyama M. Performance of reinforced soil structures during the 1995 Hyogo-ken Nambu Earthquake. In: H. Ochiai, N. Yasufuku, K. Omine, editors. Earth reinforcement, vol. 2. Rotterdam: Balkema; 1997. p. 979–1008.
[30] Tatsuoka F, Koseki J, Tateyama M, Munaf Y, Horii K. Seismic stability against high seismic loads of geosynthetic reinforced soil retaining structures. Proceedings of the Sixth International Conference on Geosynthetics, Atlanta, Georgia, vol. 1.; 1998. p. 103–41.
[31] Veletsos AS, Younan AH. Dynamic response of cantilever retaining walls. J Geotech Geoenviron Engng, ASCE 1997;123:161–72.
[32] Werners, editor. Seismic guidelines for ports, ASCE-TCLEE monograph No. 12; 1998.
[33] Wood JH. Earthquake-induced pressures on a rigid wall structure. Bull N Z Natl Earthquake Engng 1975;8:175–86.